RESEARCH ARTICLE

Metabolic phenotypes in triple-negative breast cancer

Sewha Kim · Do Hee Kim · Woo-Hee Jung ·
Ja Seung Koo

Abstract The aim of study was to investigate the metabolism of tumor and stromal cells necessary to determine differential tumor–stroma metabolic interactions according to the molecular subtypes of triple-negative breast cancer (TNBC). Tissues from 132 patients of TNBC were prepared for use as tissue microarrays (TMA). Expression of CK5/6, EGFR, claudin 3, claudin 4, claudin7, E-cadherin, AR, GGT1, STAT1, and interleukin-8 was evaluated by immunohistochemical staining using TMA to classify molecular subtypes of TNBC. In addition, immunohistochemical staining for Glut1, CAIX, BNIP3, MCT4, Beclin-1, LC3A, LC3B, and p62 was performed. According to glycolytic status determined by the immunohistochemical expression of Glut-1 and CAIX in tumor and stroma, the metabolic phenotypes of the TNBCs were defined as follows: Warburg type (tumor: glycolysis, stroma: non-glycolysis), reverse Warburg type (tumor: non-glycolysis, stroma: glycolysis), mixed metabolic type (tumor: glycolysis, stroma: glycolysis), and metabolic null type (tumor: non-glycolysis, stroma: non-glycolysis). TNBCs were classified as follows: 79 Warburg type (59.8 %), 7 reverse Warburg type (5.3 %), 24 mixed metabolic type (18.2 %), and 22 metabolic null type (16.7 %). There was no statistical significance between the metabolic phenotypes and molecular subtypes ($P=0.706$). Reverse Warburg type showed the most dysfunctional mitochondrial status for stromal cells, while Warburg type showed the most functional mitochondrial status ($P=0.036$). Regarding stromal autophagy status, reverse Warburg type showed the most activated status, while all of the Warburg and metabolic null types showed a non-activated status ($P<0.001$). In conclusion, Warburg type was the most common metabolic phenotype in TNBC, while reverse Warburg type was the most unusual. Metabolic phenotypes did not differ among the molecular subtypes of TNBCs.

Keywords Breast cancer · Reverse Warburg effect · Triple negative · Warburg effect

Introduction

Metabolism in malignant tumors is usually described by the Warburg effect, an observation that cancer cells produce energy by glycolysis rather than by oxidative phosphorylation (OXPHOS) [1]. Breast cancer is a representative tumor that shows stromal heterogeneity, and tumor–stroma interaction plays an important role in tumor growth and progression. Therefore, there is a chance of such an interaction in tumor metabolism. A previous study indicated a metabolic interaction between breast cancer cells and stromal cells, the so-called reverse Warburg effect [2–5]. Briefly, reactive oxygen species such as nitric oxide generated by breast cancer cells impose oxidative stress and induce glycolysis, autophagy (mitophagy), and mitochondria dysfunction in stromal cells via activation of HIF-1α and NFκB. The products of glycolysis, such as ketone bodies and lactate, are transported to adjacent cancer cells and incorporated into OXPHOS to generate ATP, thereby contributing to the tumor growth and progression. Cancer-associated fibroblasts are known to be caveolin-1-deficient stromal cells that interact with breast cancer cells. Loss of caveolin-1 expression is the result of increased autophagic degradation of caveolin-1 protein [3,5–7]. Table 1 shows the dominant metabolism, mitochondrial status, and autophagy status of each compartment in the Warburg effect and reverse Warburg effect, respectively.

S. Kim · D. H. Kim · W.-H. Jung
Department of Pathology, Yonsei University Health System,
Seoul, South Korea

J. S. Koo (✉)
Department of Pathology, Yonsei University College of Medicine,
Severance Hospital, 50 Yonsei-ro Seodaemun-gu,
Seoul 120-752, South Korea
e-mail: kjs1976@yuhs.ac

Table 1 Comparison of metabolism type, mitochondrial status, and autophagy status between Warburg effect theory and reverse Warburg effect theory

Metabolism theory	Warburg effect theory	Reverse Warburg effect theory	
Site	Cancer cell	Cancer cell	Stromal cell
Metabolism	Glycolysis	OXPHOS	Glycolysis
Mitochondrial status	Dysfunctional	Functional	Dysfunctional
Autophagy status	n/a	Not activated	Activated

OXPHOS oxidative phosphorylation, *n/a* not available

Breast cancer is a representative heterogeneous tumor in its clinical, histological, and molecular genetic signatures. Through studies performed to categorize breast cancers into subtypes with similar signatures, five molecular subtypes (luminal A, luminal B, HER-2, normal breast-like, and basal-like type) were identified [8–10]. Aside from the five subtypes defined by their gene expression profiles, breast cancers not expressing estrogen receptor (ER), progesterone receptor (PR), or human epidermal growth factor receptor 2 (HER2) are referred to as triple-negative breast cancer (TNBC) [11]. TNBC constitutes a heterogeneous group of breast cancer for which no effective targeted therapies are known due to its lack of ER, PR, and HER2 expression. TNBC can be subclassified into basal-like type, molecular-apocrine type, and claudin-low type groups based upon the results of gene profiling studies [12]. TNBC is typically characterized by high histologic grade, tumor necrosis, frequent mitosis, aggressive biologic behavior, and poor prognosis. These features of TNBC are similar to those of tumors with high metabolic activity [13–16]. Indeed, tumors with high metabolic activity have been previously characterized by high histologic grade, high proliferation, poor differentiation, and poor prognosis [17–20]. Accordingly, high metabolic activity is expected in triple-negative breast cancer. In the previous study [21], we identified that TNBC (especially basal-like TNBC) exhibited the highest Glut-1 and CAIX expression among the molecular subtypes of breast cancer. Glut-1 and CAIX are major molecules involved in aerobic glycolysis [22]. In short, Glut-1 facilitates glucose transport across the cell membrane, and the intracellular transfer of glucose increases with the elevation of Glut-1 expression. Lactate overproduction during enhanced glycolysis leads to intracellular acidosis, which in turn increases the expression of carbonic anhydrase IX (CAIX), a pH regulator [22]. Therefore, the Warburg type metabolism could be considered an important metabolic phenotype of basal-like TNBC. As an extension of the previous study, we intended to further classify TNBC and then examine the expression of glycolytic-related proteins in the tumor and stroma compartment to determine the dominant metabolic phenotypes according to the TNBC subtypes.

The purpose of this study was to investigate the metabolism type, mitochondrial status, and autophagy status in tumor and stromal cells in order to determine the difference of tumor–stroma metabolic interactions according to TNBC molecular subtype.

Materials and methods

Patient selection

Patients who were diagnosed with TNBC and underwent surgical excision at Severance Hospital between January 2000 and December 2005 were included in the study group. Patients who received preoperative hormonal therapy or neoadjuvant chemotherapy were excluded. There were 132 TNBC cases included. This study was approved by the Institutional Review Board of Yonsei University Severance Hospital. TNBC was defined when breast cancer was negative for ER, PR, and HER2 by immunohistochemical staining as well as for HER2 amplification by fluorescence in situ hybridization (FISH). ER and PR immunohistochemistry signals were considered positive when they were expressed in more than 1 % of invasive tumor cells [23]. HER2 staining was scored according to the American Society of Clinical Oncology (ASCO)/College of American Pathologists (CAP) guideline using the following categories: 0, no immunostaining; 1+, weak incomplete membranous staining in any proportion of tumor cells; 2+, complete membranous staining, either non-uniform or weak in at least 10 % of tumor cells; and 3+, uniform intense membranous staining in >30 % of tumor cells [24]. Cases with 0 to 1+ were regarded as negative, and cases with 3+ were considered positive. Cases with HER-2 2+ were investigated with FISH (Vysis pathvision HER-2 kit) for HER-2 gene status. As proposed by the ASCO/CAP guideline, an absolute HER-2 gene copy number lower than 4 or HER-2 gene/chromosome 17 copy number ratio (HER-2/Chr17 ratio) of less than 1.8 was considered HER-2 negative; an absolute HER-2 copy number between 4 and 6 or HER-2/Chr17 ratio between 1.8 and 2.2 was considered HER-2 equivocal; and an absolute HER2 copy number greater than 6 or HER-2/Chr17 ratio higher than 2.2 was considered HER-2-positive [24]. All hematoxylin and eosin (H&E)-stained slides for each case were retrospectively reviewed by breast pathologists (Koo JS). The histological grade was assessed using the Nottingham grading system [25]. Histologic findings including apocrine histology, central fibrotic zone, and lymphocyte infiltration were evaluated in all cases. The apocrine histology was defined when abundant granular eosinophilic cytoplasm, cytoplasmic vacuolization, and vesicular nuclei with prominent nucleoli were present in more than 10 % of tumor cells. Clinicopathologic

parameters evaluated in each breast cancer included patient age at initial diagnosis, lymph node metastasis, tumor recurrence, distant metastasis, and patient survival.

Tissue microarray

On H&E-stained slides of tumors, a representative area was selected, and a corresponding spot was marked on the surface of a paraffin block. Using a punch machine, the representative area of the tumor was punched out and a 3-mm tissue core was placed into a 6×5 recipient block. Tissue of invasive tumors was then extracted. Two tissue cores were extracted to minimize extraction bias. Each tissue core was assigned a unique tissue microarray location number that was linked to a database containing additional clinicopathological data.

Immunohistochemistry

The antibodies used for immunohistochemistry in this study are shown in Table 2. All immunohistochemical staining was performed on formalin-fixed, paraffin-embedded tissue sections. Briefly, 5-μm-thick sections were obtained with a microtome, transferred onto adhesive slides, and dried at 62 °C for 30 min. After incubation with primary antibodies,

immunodetection was performed with biotinylated anti-mouse immunoglobulin, followed by peroxidase-labeled streptavidin using a labeled streptavidin biotin kit with 3,3′-diaminobenzidine chromogen as the substrate. The primary antibody incubation step was omitted in the negative control. Slides were counterstained with Harris hematoxylin.

Interpretation of immunohistochemical staining

All immunohistochemical markers were accessed by light microscopy. Glut1, CAIX, BNIP3, MCT4, Beclin-1, LC3A, LC3B, and p62 immunohistochemical staining results were evaluated based on the proportion of stained cells and the immunostaining intensity. The proportion of stained cells was graded from 0 through 2 (0, negative; 1, positive in less than 30 %; and 2, positive in more than 30 % of tumor cells). Immunostaining intensity was graded from 0 through 3 (0, negative; 1, weak; 2, moderate; and 3, strong). The scores for the proportion of stained cells and the staining intensity were multiplied to provide a total score: negative (0–1) or positive (2–6). The Ki-67 labeling index was defined as the percentage of tumor cells exhibiting nuclear staining versus the total number of tumor cells. Immunohistochemical staining results for EGFR and CK5/6 were considered positive when expressed in more than 1 % of tumor cells. The CD20 index

Table 2 Source, clone, and dilution of antibodies used in this study

Antibody	Clone	Dilution	Company
Molecular subtype related			
Cytokeratin 5/6	D5/16B4	1:50	DAKO, Glostrup, Denmark
EGFR	EGFR.25	1:50	Novocastra, Newcastle, UK
Claudin 3	Polyclonal	1:50	Abcam, Cambridge, UK
Claudin 4	Polyclonal	1:100	Abcam, Cambridge, UK
Claudin 7	Polyclonal	1:100	Abcam, Cambridge, UK
E-cadherin	36B5	1:100	Novocastra, Newcastle, UK
Androgen receptor	AR441	1:50	DAKO, Glostrup, Denmark
GGT1	IgG2A	1:50	Abcam, Cambridge, UK
Ki-67	MIB-1	1:150	DAKO, Glostrup, Denmark
STAT1	Polyclonal	1:100	Abcam, Cambridge, UK
Interleukin-8	807	1:50	Abcam, Cambridge, UK
Glycolysis related			
Glut-1	SPM498	1:200	Abcam, Cambridge, UK
CAIX	Polyclonal	1:100	Abcam, Cambridge, UK
MCT4	Polyclonal	1:100	Santa cruz, California, USA
Mitochondrial status related			
BNIP3	Ana40	1:100	Abcam, Cambridge, UK
Autophagy related			
Beclin-1	Polyclonal	1:100	Abcam, Cambridge, UK
LC3A	EP1528Y	1:100	Abcam, Cambridge, UK
LC3B	Polyclonal	1:100	Abcam, Cambridge, UK
p62	SQSTM1	1:100	Abcam, Cambridge, UK

was defined by the percentage of area infiltrated by CD20-positive lymphocyte to entire area including both the tumor and surrounding stroma.

Molecular classification of TNBC according to IHC

According to immunohistochemistry results, the TNBC specimens were subclassified as either basal-like type (CK5/6 positive and/or EGFR positive), molecular apocrine type (AR positive and/or GGT1 positive), claudin low type (claudin 3, claudin 4, claudin 7 negative, and/or E-cadherin negative), immune-related type (STAT1 positive and IL-8 negative), mixed type (features of more than two types), or null type (none of the above).

Classification of tumor metabolic subtype

In this study, TNBCs were categorized into the following categories according to the immunohistochemical staining results of metabolism-related proteins (Fig. 1): glycolysis type: positive for Glut1 and/or CAIX; non-glycolysis type: negative for Glut1 and CAIX; dysfunctional mitochondria status: positive for BNIP; functional mitochondria: negative for BNIP3; activated autophagy status: positive for more than two among beclin-1, LC3A, LC3B, and p62; and non-activated autophagy status: positive for less than two among beclin-1, LC3A, LC3B, and p62.

Metabolic phenotypes were defined as follows: Warburg type, when the tumor exhibited a glycolysis signature while the stroma did not; reverse Warburg type, when the tumor exhibited a non-glycolysis signature while the stroma exhibited a glycolysis signature; mixed metabolic type, when both the tumor and stroma exhibited a glycolysis signature; and metabolic null type, when neither the tumor nor stroma exhibited a glycolysis signature.

MCT4, GLUT-1, and CAIX are proteins involved in glycolysis. Although there was a significant correlation between the GLUT-1 and CAIX expression [21,26], MCT4 expression had no correlation with GLUT-1/CAIX expression. Thus, the metabolic phenotype was defined by GLUT-1 and CAIX expression, not by MCT4 expression in this study.

Statistical analysis

Data were processed using SPSS for Windows, version 12.0 (SPSS Inc., Chicago, IL, USA). Student's t and Fisher's exact tests were used to examine any difference in continuous and categorical variables, respectively. Significance was assumed when $P < 0.05$. Kaplan–Meier survival curves and log-rank statistics were employed to evaluate time to tumor metastasis and time to survival. Multivariate regression analysis was performed using Cox proportional hazards model.

Results

Clinicopathological characteristics according to molecular subtype of TNBC are shown in Table 3. In total, 132 TNBCs were classified into subtypes, including 55 basal-like type (41.7 %), 11 molecular apocrine type (8.3 %), 8 claudin-low type (6.1 %), 6 immune-related type (4.5 %), 29 mixed type (22.0 %), and 23 null type (17.4 %).

The 29 mixed TNBCs included 9 basal-like + claudin low, 8 basal-like + immune related, and 7 basal-like + molecular
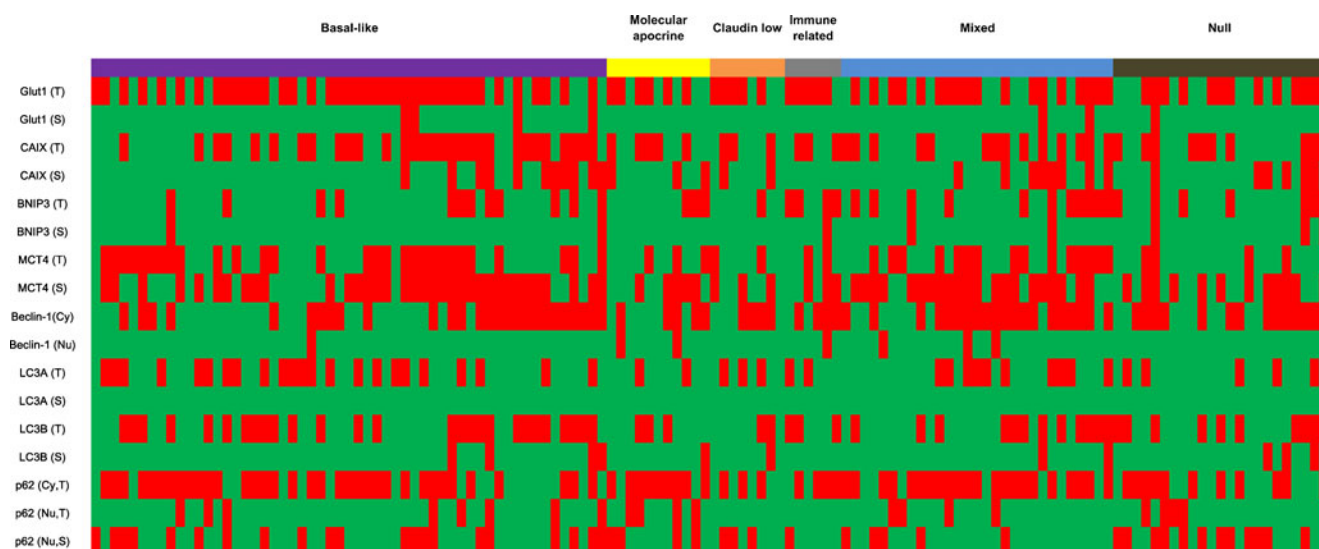

Fig. 1 A heatmap representing status of metabolism-related proteins in tumor and stroma according to the molecular subtype of triple-negative breast cancer. *T* tumor, *S* stroma, *Cy* cytoplasm, *Nu* nucleus, *Red* positive, *Green* negative

Table 3 Clinicopathologic characteristics of patients according to TNBC phenotype

Parameters	Total (n=132) (%)	Basal-like type (n=55) (%)	Molecular apocrine type (n=11) (%)	Claudine low type (n=8) (%)	Immune related type (n=6) (%)	Mixed type (n=29) (%)	Null type (n=23) (%)	P value
Age (years, mean±SD)	48.3±12.4	46.9±11.2	51.3±15.4	49.8±8.2	52.3±18.7	48.9±12.8	48.1±13.2	0.833
Histologic grade								0.586
I/II	42 (31.8)	17 (30.9)	6 (54.5)	3 (37.5)	1 (16.7)	9 (31.0)	9 (26.1)	
III	90 (68.2)	38 (69.1)	5 (45.5)	5 (62.5)	5 (83.3)	20 (69.0)	17 (73.9)	
Tumor stage								0.719
T1	50 (37.9)	24 (43.6)	5 (45.5)	3 (37.5)	1 (16.7)	10 (34.5)	7 (30.4)	
T2/T3	82 (62.1)	31 (56.4)	6 (54.5)	5 (62.5)	5 (83.3)	19 (65.5)	16 (69.6)	
Nodal stage								0.459
N0	86 (65.2)	40 (72.7)	6 (54.5)	5 (62.5)	5 (83.3)	18 (62.1)	12 (52.2)	
N1/N2/N3	46 (34.8)	15 (27.3)	5 (45.5)	3 (37.5)	1 (16.7)	11 (37.9)	11 (47.8)	
Central acellular zone								0.224
No	101 (76.5)	38 (69.1)	11 (100.0)	6 (75.0)	6 (100.0)	22 (75.9)	18 (78.3)	
Yes	31 (23.5)	17 (30.9)	0 (0.0)	2 (25.0)	0 (0.0)	7 (24.1)	5 (21.7)	
Central necrotic zone								0.877
No	123 (93.2)	51 (92.7)	11 (100.0)	7 (87.5)	6 (100.0)	27 (93.1)	21 (91.3)	
Yes	9 (6.8)	4 (7.3)	0 (0.0)	1 (12.5)	0 (0.0)	2 (6.9)	2 (8.7)	
Central fibrotic zone								0.351
No	106 (80.3)	41 (74.5)	11 (100.0)	6 (75.0)	6 (100.0)	23 (79.3)	19 (82.6)	
Yes	26 (19.7)	14 (25.5)	0 (0.0)	2 (25.0)	0 (0.0)	6 (20.7)	4 (17.4)	
Lymphocytic infiltration								0.025
Absent	99 (75.0)	41 (74.5)	8 (72.7)	7 (87.5)	2 (33.3)	19 (65.5)	22 (95.7)	
Present	33 (25.0)	14 (25.5)	3 (27.3)	1 (12.5)	4 (66.7)	10 (34.5)	1 (4.3)	
Tumor cell discohesiveness								0.082
No	122 (92.4)	53 (96.4)	8 (72.7)	7 (87.5)	6 (100.0)	28 (96.6)	20 (87.0)	
Yes	10 (7.6)	2 (3.6)	3 (27.3)	1 (12.5)	0 (0.0)	1 (3.4)	3 (13.0)	
Tumor margin								0.165
Expanding	112 (84.8)	49 (89.1)	8 (72.7)	7 (87.5)	6 (100.0)	26 (89.7)	16 (69.6)	
Infiltrative	20 (15.2)	6 (10.9)	3 (27.3)	1 (12.5)	0 (0.0)	3 (10.3)	7 (30.4)	
Apocrine differentiation								0.026
No	108 (81.8)	47 (85.5)	5 (45.5)	7 (87.5)	4 (66.7)	24 (82.8)	21 (91.3)	
Yes	24 (18.2)	8 (14.5)	6 (54.5)	1 (12.5)	2 (33.3)	5 (17.2)	2 (8.7)	
Tumor cell necrosis (%, mean±SD)	9.5±14.0	9.3±13.0	7.2±14.2	6.9±7.9	6.6±10.3	11.2±16.9	10.4±15.5	0.934
Ki67 LI (%, mean±SD)	27.3±23.3	33.3±24.6	6.0±4.8	27.3±27.8	38.6±27.5	28.5±22.4	20.7±17.4	0.005
CD20 index (mean±SD)	2.4±6.3	0.9±2.1	3.8±9.1	2.1±5.2	3.3±4.0	2.3±3.7	5.2±11.9	0.146
Tumor recurrence	14 (10.6)	7 (12.7)	1 (9.1)	1 (12.5)	0 (0.0)	1 (3.4)	4 (17.4)	0.591
Patient death	14 (10.6)	7 (12.7)	1 (9.1)	1 (12.5)	1 (16.7)	0 (0.0)	4 (17.4)	0.403
Duration of clinical follow-up (months, mean±SD)	56.4±21.9	57.7±22.8	63.7±23.7	63.3±17.6	52.1±29.1	50.0±20.3	56.3±20.2	0.436

TNBC triple-negative breast cancer

Table 4 Status of metabolism-related proteins according to TNBC phenotype

Parameters	Total (n=132) (%)	Basal-like type (n=55) (%)	Molecular apocrine type (n=11) (%)	Claudine low type (n=8) (%)	Immune related type (n=6) (%)	Mixed type (n=29) (%)	Null type (n=23) (%)	P value
Glut 1 in tumor								0.681
Negative	46 (34.8)	16 (29.1)	5 (45.5)	3 (37.5)	1 (16.7)	11 (37.9)	10 (43.5)	
Positive	86 (65.2)	39 (70.9)	6 (54.5)	5 (62.5)	5 (83.3)	18 (62.1)	13 (56.5)	
Glut1 in stroma								0.753
Negative	125 (94.5)	51 (92.7)	11 (100.0)	8 (100.0)	6 (100.0)	27 (93.1)	22 (95.7)	
Positive	7 (5.3)	4 (7.3)	0 (0.0)	0 (0.0)	0 (0.0)	2 (6.9)	1 (4.3)	
CAIX in tumor								0.920
Negative	67 (50.8)	25 (45.5)	6 (54.5)	5 (62.5)	3 (50.0)	15 (51.7)	13 (56.5)	
Positive	65 (49.2)	30 (54.5)	5 (45.5)	3 (37.5)	5 (50.0)	14 (48.3)	10 (43.5)	
CAIX in stroma								0.748
Negative	102 (77.3)	44 (80.0)	8 (72.7)	6 (75.0)	6 (100.0)	21 (72.4)	17 (73.9)	
Positive	30 (22.7)	11 (20.0)	3 (27.3)	2 (25.0)	0 (0.0)	8 (27.6)	6 (26.1)	
BNIP3 in tumor								0.170
Negative	94 (71.2)	43 (78.2)	8 (72.7)	7 (87.5)	2 (33.3)	18 (62.1)	16 (69.6)	
Positive	38 (28.8)	12 (21.8)	3 (27.3)	1 (12.5)	4 (66.7)	11 (37.9)	7 (30.4)	
BNIP3 in stroma								0.418
Negative	124 (93.9)	53 (96.4)	11 (100.0)	8 (100.0)	5 (83.3)	27 (93.1)	20 (87.0)	
Positive	8 (6.1)	2 (3.6)	0 (0.0)	0 (0.0)	1 (16.7)	2 (6.9)	3 (13.0)	
MCT4 in tumor								0.041
Negative	77 (58.3)	26 (47.3)	8 (72.7)	6 (75.0)	4 (66.7)	14 (48.3)	19 (82.6)	
Positive	55 (41.7)	29 (52.7)	3 (27.3)	2 (25.0)	2 (33.3)	15 (51.7)	4 (17.4)	
MCT4 in stroma								0.342
Negative	53 (40.2)	20 (36.4)	6 (54.5)	5 (62.5)	3 (50.0)	8 (27.6)	11 (47.8)	
Positive	79 (59.8)	35 (63.6)	5 (45.5)	3 (37.5)	3 (50.0)	21 (72.4)	12 (52.2)	
Cytoplasmic beclin-1								0.527
Negative	58 (43.9)	28 (50.9)	6 (54.5)	4 (50.0)	2 (33.3)	9 (31.0)	9 (39.1)	
Positive	74 (56.1)	27 (49.1)	5 (45.5)	4 (50.0)	4 (66.7)	20 (69.0)	14 (60.9)	
Nuclear beclin-1								0.084
Negative	125 (94.7)	54 (98.2)	9 (81.8)	8 (100.0)	5 (83.3)	26 (89.7)	23 (100.0)	
Positive	7 (5.3)	1 (1.8)	2 (18.2)	0 (0.0)	1 (16.7)	3 (10.3)	0 (0.0)	
LC3A in tumor								0.506
Negative	87 (65.9)	32 (58.2)	9 (81.8)	5 (62.5)	4 (66.7)	19 (65.5)	18 (78.3)	
Positive	45 (34.1)	23 (41.8)	2 (18.2)	3 (37.5)	2 (33.3)	10 (34.5)	5 (21.7)	
LC3A in stroma								n/a
Negative	132 (100.0)	55 (100.0)	11 (100.0)	8 (100.0)	6 (100.0)	29 (100.0)	23 (100.0)	
Positive	0 (0.0)	0 (0.0)	0 (0.0)	0 (0.0)	0 (0.0)	0 (0.0)	0 (0.0)	
LC3B in tumor								0.677
Negative	75 (56.8)	28 (50.9)	8 (72.7)	6 (75.0)	3 (50.0)	17 (58.6)	13 (56.5)	
Positive	57 (43.2)	27 (49.1)	3 (27.3)	2 (25.0)	3 (50.0)	12 (41.4)	10 (43.5)	
LC3B in stroma								0.906

Table 4 (continued)

Parameters	Total (n=132) (%)	Basal-like type (n=55) (%)	Molecular apocrine type (n=11) (%)	Claudine low type (n=8) (%)	Immune related type (n=6) (%)	Mixed type (n=29) (%)	Null type (n=23) (%)	P value
Negative	121 (91.7)	51 (92.7)	10 (90.9)	7 (87.5)	6 (100.0)	27 (93.1)	20 (87.0)	
Positive	11 (8.3)	4 (7.3)	1 (9.1)	1 (12.5)	0 (0.0)	2 (6.9)	3 (13.0)	0.140
Cytoplasmic p62 in tumor								
Negative	48 (36.4)	20 (36.4)	2 (18.2)	5 (62.5)	2 (33.3)	7 (24.1)	12 (52.2)	
Positive	84 (63.6)	35 (63.6)	9 (81.8)	3 (37.5)	4 (66.7)	22 (75.9)	11 (47.8)	0.261
Nuclear p62 in tumor								
Negative	112 (84.8)	47 (85.5)	7 (63.6)	8 (100.0)	6 (100.0)	25 (86.2)	19 (82.6)	
Positive	20 (15.2)	8 (14.5)	4 (36.4)	0 (0.0)	0 (0.0)	4 (13.8)	4 (17.4)	0.147
Nuclear p62 in stroma								
Negative	86 (65.2)	34 (61.8)	7 (63.6)	5 (62.5)	5 (83.3)	24 (82.8)	11 (47.8)	
Positive	46 (34.8)	21 (38.2)	4 (36.4)	3 (37.5)	1 (16.7)	5 (17.2)	12 (52.2)	

apocrine type tumors. Clinicopathologic factors associated with TNBC molecular subtype were lymphocytic infiltration ($P=0.025$), apocrine differentiation ($P=0.025$), and Ki-67 L.I. ($P=0.005$). Lymphocytic infiltration was most conspicuous in immune-related type and least in metabolic null type. Apocrine differentiation was most frequently observed in molecular apocrine type and least in metabolic null type. Ki-67 L.I was highest in immune-related type and lowest in molecular apocrine type.

Expression of metabolism-related proteins according to TNBC phenotype

Metabolism-related protein expression according to the molecular subtype of TNBC is summarized in Table 4, Figs. 1 and 2. Tumoral expression of MCT4 differed between the molecular subtypes of TNBC ($P=0.041$), which was highest for the basal-like type and lowest for the metabolic null type. Even though not statistically significant, tumoral BNIP3 expression was highest in immune-related type ($P=0.170$), while nuclear beclin-1 and cytoplasmic p62 expressions were highest in molecular apocrine type ($P=0.084$ and $P=0.140$, respectively). Nuclear p62 expression in the stroma was highest in null type ($P=0.147$).

Clinicopathologic characteristics of patients according to metabolic phenotype in TNBC

Clinicopathological characteristics according to the metabolic phenotype of TNBC are shown in Table 5. TNBCs were classified into metabolic phenotypes, including 79 Warburg type (59.8 %), 7 reverse Warburg type (5.3 %), 24 mixed metabolic type (18.2 %), and 22 metabolic null type (16.7 %). Patients with Warburg type tended to be younger ($P=0.039$). Metabolic phenotype-associated factors were tumor cell discohesiveness ($P=0.016$), stromal mitochondrial status ($P=0.036$), tumoral autophagy status ($P=0.044$), and stromal autophagy status ($P<0.001$). Tumor cell discohesiveness was most frequently observed in metabolic null type and never in mixed metabolic type. As for stromal mitochondrial status, reverse Warburg type showed the most dysfunctional status, while Warburg type showed the most functional status. As for tumoral autophagy status, mixed metabolic type showed the most activated status, while metabolic null type showed the least activated status. With respect to stromal autophagy status, reverse Warburg type showed the most activated status, while all of the Warburg and metabolic null type showed non-activated status.

Although there was no significant association between the metabolic phenotype and molecular subtype, we determined each molecular subtypes' metabolic phenotype in order of frequency (1) basal-like type: Warburg type→mixed metabolic type→metabolic null type→reverse Warburg type; (2)
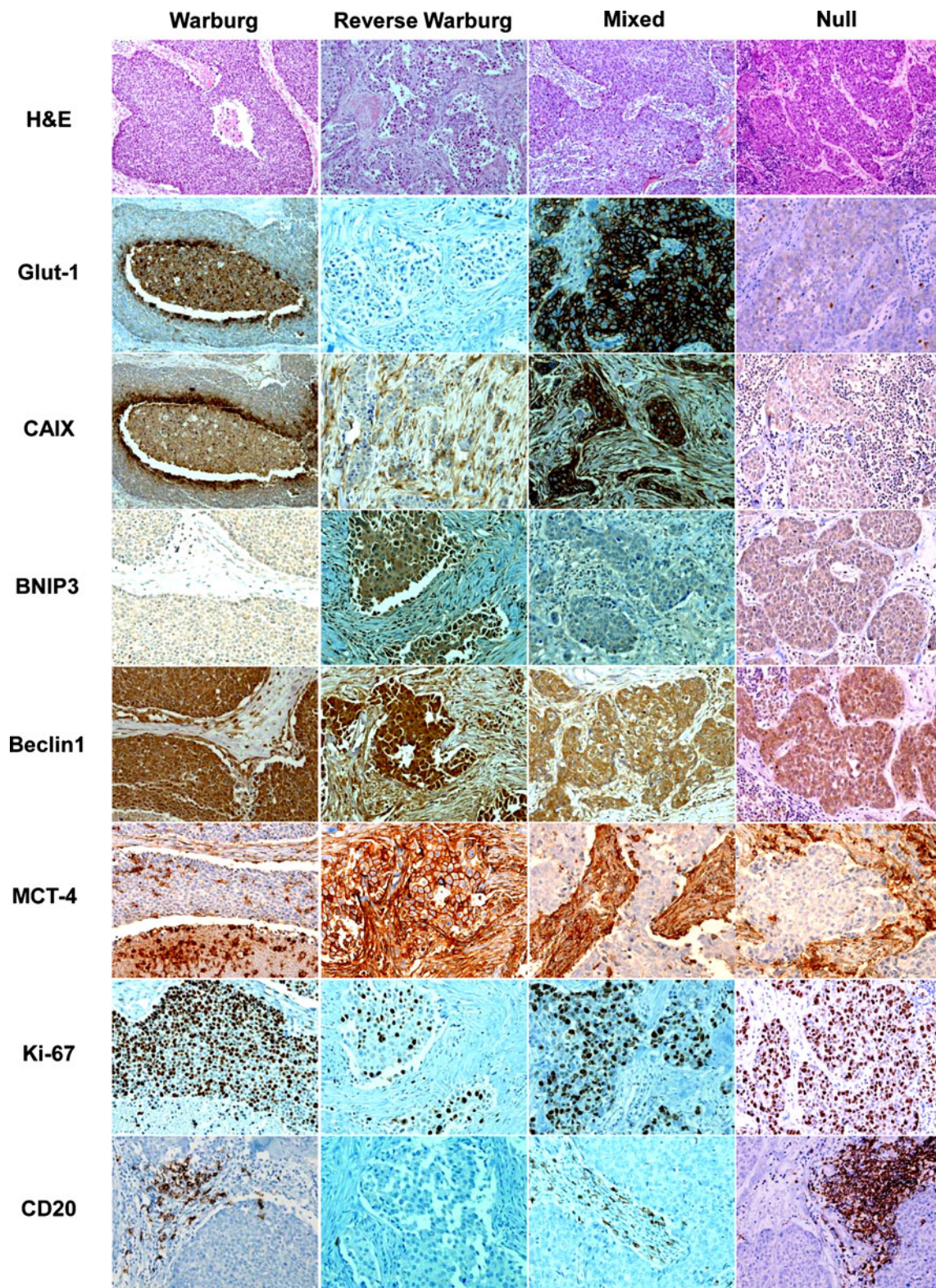
Fig. 2 Histologic and immunohistochemical features according to the metabolic phenotypes of triple-negative breast cancer. Warburg type shows expression of Glut-1 and CAIX in tumor, but reverses Warburg type in stroma, mixed metabolic type in tumor and stroma, and metabolic null type in neither tumor nor stroma. Reverse Warburg type reveals expression of BNIP3 and beclin1 in stroma, but lower Ki-67 labeling index and CD20 positive B cell than other types

Table 5 Clinicopathologic characteristics of patients according to metabolic phenotype

Parameters	Warburg type (n=79) (%)	Reverse Warburg type (n=7) (%)	Mixed metabolic type (n=24) (%)	Metabolic null type (n=22) (%)	P value
Age (years, mean±SD)	45.8±11.9	53.1±13.6	51.9±10.0	52.1±14.4	0.039
Histologic grade					0.109
I/II	23 (29.1)	5 (71.4)	6 (25.0)	8 (36.4)	
III	56 (70.9)	2 (28.6)	18 (75.0)	14 (63.6)	
Tumor stage					0.244
T1	25 (31.6)	3 (42.9)	13 (54.2)	9 (40.9)	
T2/T3	54 (68.4)	4 (57.1)	11 (45.8)	13 (59.1)	
Nodal stage					0.113
N0	53 (67.1)	3 (42.9)	19 (79.2)	11 (50.0)	
N1/N2/N3	26 (32.9)	4 (57.1)	5 (20.8)	11 (50.0)	
Central acellular zone					0.730
No	61 (77.2)	6 (85.7)	19 (79.2)	15 (68.2)	
Yes	18 (22.8)	1 (14.3)	5 (20.8)	7 (31.8)	
Central necrotic zone					0.848
No	74 (93.7)	7 (100.0)	22 (91.7)	20 (90.9)	
Yes	5 (6.3)	0 (0.0)	2 (8.3)	2 (9.1)	
Central fibrotic zone					0.960
No	64 (81.0)	6 (85.7)	19 (79.2)	17 (77.3)	
Yes	15 (19.0)	1 (14.3)	5 (20.8)	5 (22.7)	
Lymphocytic infiltration					0.116
Absent	54 (68.4)	6 (85.7)	22 (91.7)	17 (77.3)	
Present	25 (31.6)	1 (14.3)	2 (8.3)	5 (22.7)	
Tumor cell discohesiveness					0.016
No	75 (94.9)	6 (85.7)	24 (100.0)	17 (77.3)	
Yes	4 (5.1)	1 (14.3)	0 (0.0)	5 (22.7)	
Tumor margin					0.120
Expanding	68 (86.1)	5 (71.4)	23 (95.8)	16 (72.7)	
Infiltrative	11 (13.9)	2 (28.6)	1 (4.2)	6 (27.3)	
Apocrine differentiation					0.172
No	69 (87.3)	5 (71.4)	19 (79.2)	15 (68.2)	
Yes	10 (12.7)	2 (28.6)	5 (20.8)	7 (31.8)	
Cancer phenotype					0.706
Basal-like type	35 (44.3)	2 (28.6)	10 (41.7)	8 (36.4)	
Molecular apocrine type	6 (7.6)	2 (28.6)	1 (4.2)	2 (9.1)	
Claudin low type	4 (5.1)	0 (0.0)	2 (8.3)	2 (9.1)	
Immune related type	6 (7.6)	0 (0.0)	0 (0.0)	0 (0.0)	
Mixed type	16 (20.3)	1 (14.3)	7 (29.2)	5 (22.7)	
Null type	12 (15.2)	2 (28.6)	4 (16.7)	5 (22.7)	
Tumor mitochondria status					0.312
Dysfunctional	21 (26.6)	4 (57.1)	8 (33.3)	5 (22.7)	
Functional	58 (73.4)	3 (42.9)	16 (66.7)	17 (77.3)	
Stroma mitochondria status					0.036
Dysfunctional	2 (2.5)	2 (28.6)	2 (8.3)	2 (9.1)	
Functional	77 (97.5)	5 (71.4)	22 (91.7)	20 (90.9)	
Tumor autophagy status					0.044
Activated	55 (69.9)	4 (57.1)	20 (83.3)	10 (45.5)	
Non-activated	24 (30.4)	3 (42.9)	4 (16.7)	12 (54.5)	
Stroma autophagy status					<0.001

Table 5 (continued)

Parameters	Warburg type (n=79) (%)	Reverse Warburg type (n=7) (%)	Mixed metabolic type (n=24) (%)	Metabolic null type (n=22) (%)	P value
Activated	0 (0.0)	2 (28.6)	2 (8.3)	0 (0.0)	
Non-activated	79 (100.0)	5 (71.4)	22 (91.7)	22 (100.0)	
MCT4 in tumor					0.395
Negative	46 (58.2)	2 (28.6)	15 (62.5)	14 (63.6)	
Positive	33 (41.8)	5 (71.4)	9 (37.5)	8 (36.4)	
MCT4 in stroma					0.321
Negative	32 (40.5)	2 (28.6)	7 (29.2)	12 (54.5)	
Positive	47 (59.5)	5 (71.4)	17 (70.8)	10 (45.5)	
Tumor cell necrosis					
(%, mean±SD)	10.0±14.3	0.0±0.0	11.0±14.1	9.0±14.4	0.308
Ki-67 LI (%, mean±SD)	27.4±24.6	18.7±14.1	32.7±19.6	26.0±24.9	0.518
CD20 index (mean±SD)	2.0±4.3	0.1±0.3	2.1±6.1	5.0±11.2	0.168
Tumor recurrence	10 (12.7)	1 (14.3)	1 (14.3)	2 (9.1)	0.670
Patient death	9 (11.4)	2 (28.6)	1 (4.2)	2 (9.1)	0.316

molecular apocrine type: Warburg type→metabolic null type and reverse Warburg type→mixed metabolic type; (3) claudin-low type: Warburg type→metabolic null type and mixed metabolic type→reverse Warburg type; (4) immune related type: only Warburg type; (5) mixed type: Warburg type→mixed metabolic type→metabolic null type→reverse Warburg type; and (6) null type: Warburg type→metabolic null type→mixed metabolic type→reverse Warburg type.

Impact of metabolism-related proteins on patient prognosis in TNBC

Univariate analysis of patient prognosis according to the expression of metabolism-related proteins indicated that there was no factor associated with shorter disease-free survival (DFS; Table 6). Even though not significant, cytoplasmic p62 expression in tumor cells was associated with shorter DFS ($P=0.066$). Shorter overall survival (OS) was significantly associated with stromal MCT4 negativity ($P=0.039$). The multivariate Cox analysis shows that younger age [≤35 vs >35, odds ratio (OR), 4.361; 95 % confidence interval (CI), 1.264–15.043, $P=0.020$] and lymph node metastasis (N0 vs N1/2/3; OR, 6.954; 95 % CI, 1.821–26.549, $P=0.005$) were significant independent factors for shorter DFS. In addition, lymph node metastasis (N0 vs N1/2/3; OR, 9.581; 95 % CI, 1.852–49.577, $P=0.007$) was a significant independent factor associated with shorter OS according to multivariate Cox analysis (Table 7).

Discussion

This study examined the difference in metabolic phenotype according to the molecular subtype of TNBC and evaluated its implications. Metabolic phenotypes in TNBC were Warburg type>mixed metabolic type>metabolic null type> reverse Warburg type in order of frequency. In this study, Warburg type was defined when the tumor exhibited a glycolysis signature and the stroma exhibited a non-glycolysis signature, and thus, our results confirmed the high glycolytic activity of tumor cells in TNBC and corresponded with the result of an earlier study which reported that glycolysis-related proteins such as Glut-1 and CAIX are highly expressed in basal-like breast cancer, which comprises the large proportion of TNBCs.

On the other hand, we found that a reverse Warburg type (defined when the tumor is non-glycolysis type and the stroma is glycolysis type) comprised the smallest proportion of TNBC. A previous study that propounded a reverse Warburg effect theory used MCF-7 cells, a well-known luminal A type breast cancer cell line as an in vitro model [6]. TNBC is distinguished from luminal type breast cancer by its molecular and clinical features. Especially, TNBC is histologically characterized by high histologic grade, poor differentiation, increased mitosis, and tumor necrosis and thus is presumed to have high metabolic activity [13–16], while luminal type usually shows a low-grade histology suggesting a different metabolic status from TNBC. In addition, glycolysis-related proteins are variably expressed depending on molecular subtype of breast cancer, according to a previous study [21], which may explain why the reverse Warburg type comprised the lowest proportion of TNBC in our study. The results obtained in our study indicated that the metabolic phenotypes did not differ considerably among the molecular subtypes of TNBC. In brief, Warburg type was the most common metabolic phenotype in all subtypes, while reverse Warburg type was the least in all molecular subtypes, except for molecular

Table 6 Univariate analysis of the expression of metabolism-related proteins in breast cancers and disease-free survival or overall survival by log-rank test

Parameters	Number of patients/recurrence/death	Disease-free survival		Overall survival	
		Mean survival (95 % CI) months	P value	Mean survival (95 % CI) months	P value
Immunohistochemical factors					
Glut 1 in tumor			0.608		0.546
Negative	46/4/6	89 (82–97)		87 (79–95)	
Positive	86/10/8	92 (86–98)		94 (89–99)	
Glut1 in stroma			n/a		n/a
Negative	125/14/14	n/a		n/a	
Positive	7/0/0	n/a		n/a	
CAIX in tumor			0.120		0.140
Negative	67/10/10	88 (81–95)		89 (82–96)	
Positive	65/4/4	97 (91–102)		97 (91–102)	
CAIX in stroma			0.449		0.981
Negative	102/12/11	92 (86–97)		93 (88–98)	
Positive	30/2/3	62 (59–65)		63 (60–67)	
BNIP3 in tumor			0.214		0.987
Negative	94/12/10	91 (85–97)		93 (87–98)	
Positive	38/2/4	84 (79–90)		82 (76–88)	
BNIP3 in stroma			n/a		n/a
Negative	124/14/14	n/a		n/a	
Positive	8/0/0	n/a		n/a	
MCT4 in tumor			0.375		0.159
Negative	77/10/11	91 (84–97)		90 (83–96)	
Positive	55/4/3	85 (79–90)		87 (83–91)	
MCT4 in stroma			0.089		0.039
Negative	53/9/10	88 (79–96)		87 (79–96)	
Positive	79/5/4	95 (91–100)		97 (93–101)	
Cytoplasmic beclin-1			0.162		0.460
Negative	58/9/8	89 (82–97)		91 (84–98)	
Positive	74/5/6	95 (90–100)		94 (89–99)	
Nuclear beclin-1			0.588		n/a
Negative	125/13/14	93 (88–98)		n/a	
Positive	7/1/0	83 (60–107)		n/a	
LC3A in tumor			0.467		0.677
Negative	87/8/10	94 (88–99)		91 (85–98)	
Positive	45/6/4	88 (80–96)		92 (86–98)	
LC3A in stroma			n/a		n/a
Negative	132/14/14	n/a		n/a	
Positive	0/0/0	n/a		n/a	
LC3B in tumor			0.436		0.412
Negative	75/9/9	91 (84–98)		91 (84–98)	
Positive	57/5/5	94 (88–100)		94 (89–100)	
LC3B in stroma			0.846		0.855
Negative	121/13/13	93 (88–97)		93 (88–97)	
Positive	11/1/1	61 (54–68)		63 (61–66)	
Cytoplasmic p62 in tumor			0.066		0.180
Negative	48/2/3	99 (94–103)		96 (89–103)	

Table 6 (continued)

Parameters	Number of patients/recurrence/death	Disease-free survival		Overall survival	
		Mean survival (95% CI) months	P value	Mean survival (95% CI) months	P value
Positive	84/12/11	88 (82–95)		90 (84–96)	
Nuclear p62 in tumor			0.913		0.538
Negative	112/12/11	93 (87–98)		93 (88–98)	
Positive	20/2/3	82 (72–93)		80 (68–91)	
Nuclear p62 in stroma			0.246		0.537
Negative	86/11/10	90 (83–96)		91 (85–97)	
Positive	46/3/4	97 (90–103)		94 (87–102)	
Tumor phenotype			n/a		n/a
Basal-like type	55/7/7	n/a		n/a	
Molecular apocrine type	11/1/1	n/a		n/a	
Claudin low type	8/1/1	n/a		n/a	
Immune related type	6/0/1	n/a		n/a	
Mixed type	29/1/0	n/a		n/a	
Null type	23/4/4	n/a		n/a	
Metabolic status			0.667		0.309
Warburg type	79/10/9	91 (84–97)		92 (86–98)	
Reverse Warburg type	7/1/2	59 (48–69)		57 (47–66)	
Mixed metabolic type	24/1/1	63 (61–66)		65 (65–65)	
Metabolic null type	22/2/2	82 (75–90)		83 (76–90)	

apocrine type. In this study, the reverse Warburg type exhibited the highest level of stromal dysfunctional mitochondria and activated stromal autophagy, while Warburg type showed the most stromal functional mitochondria and stromal non-activated autophagy, which was compatible with the results suggested by reverse Warburg effect theory [2–5].

Several metabolic-related parameters were correlated with the clinicopathologic factors in this study. First, tumoral MCT4 expression was highest in the basal-like type and lowest in the metabolic null type ($P=0.0.41$). This was in accordance with the result of a previous study, which reported that MCT1 (a member of MCT) expression was highest in

Table 7 Multivariate analysis for survival in TNBC

Parameters	Disease-free survival			Overall survival		
	Hazard ratio	95 % CI	P value	Hazard ratio	95 % CI	P value
Age (years)			0.020			0.205
≤35 vs >35	4.361	1.264–15.043		2.507	0.605–10.387	
T stage			0.272			0.597
T1 vs T2–3	3.295	0.393–27.640		1.794	0.206–15.617	
N stage			0.005			0.007
N0 vs N1–3	6.954	1.821–26.549		9.581	1.852–49.577	
Histologic grade			0.832			0.854
I/II vs III	1.143	0.332–3.934		0.882	0.232–3.351	
MCT4 in stroma			0.373			0.096
Negative vs Positive	1.709	0.526–5.548		3.866	0.787–18.996	
Cytoplasmic p62 in tumor			0.054			0.119
Negative vs positive	4.973	0.971–25.471		3.746	0.711–19.732	

TNBC triple-negative breast cancer

basal-like subtype [27]. Secondly, TNBC with Warburg metabolic phenotype was associated with younger age (P=0.039). Although there have been no previous studies about the metabolic phenotype of TNBC, renal cell carcinoma with succinate dehydrogenase (SDH) mutation occurred in younger patients as opposed to no SDH mutation. Renal cell carcinoma with SDH mutation was proposed as an aggressive example of the Warburg effect in cancer. Therefore, tumors with Warburg type metabolic phenotype are assumed to have correlation with younger age [28]. Lastly, stromal MCT4 negativity was associated with shorter OS according to the univariate analysis (P=0.039), which was a contrast to the result of the previous study which reported that stromal MCT4 expression in TNBC was a predictive factor of decreased OS [29]. MCT4 immunoexpression was graded on the 0, 1, 2, 3 scale in the previous study, which was different from the interpretive method of this study. The methodological difference could influence the conflicting results, and further study is needed to establish the MCT4 immuno-interpretation criterion.

In conclusion, Warburg type was the most common metabolic phenotype in TNBC, while reverse Warburg type was the most unusual. There was no significant difference in the metabolic phenotypes among the molecular subtypes in TNBC.

References

1. Warburg O. On the origin of cancer cells. Science. 1956;123:309–14.
2. Bonuccelli G, Tsirigos A, Whitaker-Menezes D, Pavlides S, Pestell RG, Chiavarina B, et al. Ketones and lactate "fuel" tumor growth and metastasis: evidence that epithelial cancer cells use oxidative mitochondrial metabolism. Cell Cycle. 2010;9:3506–14.
3. Martinez-Outschoorn UE, Balliet RM, Rivadeneira DB, Chiavarina B, Pavlides S, Wang C, et al. Oxidative stress in cancer associated fibroblasts drives tumor-stroma co-evolution: a new paradigm for understanding tumor metabolism, the field effect and genomic instability in cancer cells. Cell Cycle. 2010;9:3256–76.
4. Pavlides S, Tsirigos A, Vera I, Flomenberg N, Frank PG, Casimiro MC, et al. Loss of stromal caveolin-1 leads to oxidative stress, mimics hypoxia and drives inflammation in the tumor microenvironment, conferring the "reverse Warburg effect": a transcriptional informatics analysis with validation. Cell Cycle. 2010;9:2201–19.
5. Pavlides S, Whitaker-Menezes D, Castello-Cros R, Flomenberg N, Witkiewicz AK, Frank PG, et al. The reverse Warburg effect: aerobic glycolysis in cancer associated fibroblasts and the tumor stroma. Cell Cycle. 2009;8:3984–4001.
6. Martinez-Outschoorn UE, Pavlides S, Whitaker-Menezes D, Daumer KM, Milliman JN, Chiavarina B, et al. Tumor cells induce the cancer associated fibroblast phenotype via caveolin-1 degradation: implications for breast cancer and DCIS therapy with autophagy inhibitors. Cell Cycle. 2010;9:2423–33.
7. Martinez-Outschoorn UE, Trimmer C, Lin Z, Whitaker-Menezes D, Chiavarina B, Zhou J, et al. Autophagy in cancer associated fibroblasts promotes tumor cell survival: role of hypoxia, HIF1 induction and NFkappaB activation in the tumor stromal microenvironment. Cell Cycle. 2010;9:3515–33.
8. Kwon JE, Jung WH, Koo JS. Molecules involved in epithelial-mesenchymal transition and epithelial–stromal interaction in phyllodes tumors: implications for histologic grade and prognosis. Tumour Biology. 2012;33:787–98.
9. Perou CM, Sorlie T, Eisen MB, van de Rijn M, Jeffrey SS, Rees CA, et al. Molecular portraits of human breast tumours. Nature. 2000;406:747–52.
10. Sorlie T, Perou CM, Tibshirani R, Aas T, Geisler S, Johnsen H, et al. Gene expression patterns of breast carcinomas distinguish tumor subclasses with clinical implications. Proc Natl Acad Sci U S A. 2001;98:10869–74.
11. Dent R, Trudeau M, Pritchard KI, Hanna WM, Kahn HK, Sawka CA, et al. Triple-negative breast cancer: clinical features and patterns of recurrence. Clin Cancer Res. 2007;13:4429–34.
12. Perou CM. Molecular stratification of triple-negative breast cancers. Oncologist. 2011;16:61–70.
13. Reis-Filho JS, Tutt AN. Triple negative tumours: a critical review. Histopathology. 2008;52:108–18.
14. Foulkes WD, Smith IE, Reis-Filho JS. Triple-negative breast cancer. N Engl J Med. 2010;363:1938–48.
15. Venkitaraman R. Triple-negative/basal-like breast cancer: clinical, pathologic and molecular features. Expert Rev Anticancer Ther. 2010;10:199–207.
16. Rakha EA, Ellis IO. Triple-negative/basal-like breast cancer: review. Pathology. 2009;41:40–7.
17. Kato H, Takita J, Miyazaki T, Nakajima M, Fukai Y, Masuda N, et al. Glut-1 glucose transporter expression in esophageal squamous cell carcinoma is associated with tumor aggressiveness. Anticancer Res. 2002;22:2635–9.
18. Mineta H, Miura K, Takebayashi S, Misawa K, Araki K, Misawa Y, et al. Prognostic value of glucose transporter 1 expression in patients with hypopharyngeal carcinoma. Anticancer Res. 2002;22:3489–94.
19. Shaw RJ. Glucose metabolism and cancer. Curr Opin Cell Biol. 2006;18:598–608.
20. Tateishi U, Yamaguchi U, Seki K, Terauchi T, Arai Y, Hasegawa T. Glut-1 expression and enhanced glucose metabolism are associated with tumour grade in bone and soft tissue sarcomas: a prospective evaluation by [18 F]fluorodeoxyglucose positron emission tomography. Eur J Nucl Med Mol Imaging. 2006;33:683–91.
21. Choi J, Jung WH, Koo JS. Metabolism-related proteins are differentially expressed according to the molecular subtype of invasive breast cancer defined by surrogate immunohistochemistry. Pathobiology. 2013;80:41–52.
22. Semenza GL. Regulation of cancer cell metabolism by hypoxia-inducible factor 1. Semin Cancer Biol. 2009;19:12–6.
23. Hammond ME, Hayes DF, Dowsett M, Allred DC, Hagerty KL, Badve S, et al. American Society of Clinical Oncology/College Of American Pathologists guideline recommendations for immunohistochemical testing of estrogen and progesterone receptors in breast cancer. J Clin Oncol. 2010;28:2784–95.
24. Wolff AC, Hammond ME, Schwartz JN, Hagerty KL, Allred DC, Cote RJ, et al. American Society of Clinical Oncology/College of American Pathologists guideline recommendations for human epidermal growth factor receptor 2 testing in breast cancer. J Clin Oncol. 2007;25:118–45.
25. Elston CW, Ellis IO. Pathological prognostic factors in breast cancer. I. The value of histological grade in breast cancer: experience from a large study with long-term follow-up. Histopathology. 1991;19:403–10.
26. Pinheiro C, Sousa B, Albergaria A, Paredes J, Dufloth R, Vieira D, et al. GLUT1 and CAIX expression profiles in breast cancer correlate

with adverse prognostic factors and MCT1 overexpression. Histol Histopathol. 2011;26:1279–86.

27. Pinheiro C, Albergaria A, Paredes J, Sousa B, Dufloth R, Vieira D, et al. Monocarboxylate transporter 1 is up-regulated in basal-like breast carcinoma. Histopathology. 2010;56:860–7.

28. Ricketts CJ, Shuch B, Vocke CD, Metwalli AR, Bratslavsky G, Middelton L, et al. Succinate dehydrogenase kidney cancer: an aggressive example of the Warburg effect in cancer. J Urol. 2012;188:2063–71.

29. Witkiewicz AK, Whitaker-Menezes D, Dasgupta A, Philp NJ, Lin Z, Gandara R, et al. Using the "reverse Warburg effect" to identify high-risk breast cancer patients: stromal MCT4 predicts poor clinical outcome in triple-negative breast cancers. Cell Cycle. 2012;11:1108–17.